Cyclic J Integral Using Linear Matching Method

Weihang Chen, Haofeng Chen
Department of Mechanical Engineering, University of Strathclyde, Glasgow, G1 1XJ, UK

Abstract

The extended version of the latest Linear Matching Method (LMM) has the capability to evaluate the stable cyclic response, which produces cyclic stresses, residual stresses and plastic strain ranges for the low cycle fatigue assessment with cyclic load history. The objective of this study is to calculate ΔJ through the LMM and suggest future development directions. The derivation of the ΔJ based on the potential energy expression for a single edge cracked plate subjected to cyclic uniaxial loading condition using LMM is presented. To extend the analysis so that it can be incorporated to other plasticity models, material Ramberg-Osgood hardening constants are also adopted. The results of the proposed model have been compared to the ones obtained from Reference Stress Method (RSM) for a single edge cracked plate and they indicate that the estimates provide a relatively easy method for estimating ΔJ for describing the crack growth rate behaviour by considering the complete accumulated cycle effects.

Keywords: cyclic J integral; Linear Matching Method; single edge cracked plate

1. Introduction

The ability to predict crack growth continues to be an important component of research for several structural materials. Crack growth predictions can aid the understanding of the useful life of a structural component and the determination of inspection intervals and criteria. Therefore, more accurate and reliable numerical approaches for estimating crack propagation behaviour due to fatigue damage during a specified operation period are needed.

Fracture mechanics is a well known approach for predicting the crack propagation and the analysis can be based on linear-elastic or more complex elastic plastic (nonlinear) models. The cyclic *J*-integral based on the fracture mechanics was first proposed and implemented by Dowling and Begley [1] as a parameter which correlates with the crack growth rate, *da/dN*,. values of Δ*J* plotted vs. corresponding crack growth rates *da/dN*, on a double logarithmic scale, exhibited power law behaviour similar to the Paris equation [2] so that it is possible to write

$$\frac{da}{dN} = A(\Delta J)^m \qquad (1)$$

Where *A* and *m* are constants found from the least-square regression of data.

GE/EPRI and Reference Stress Method (RSM) are the simplified methods to calculate Δ*J*. It was assumed that the Δ*J* is the summation of elastic and fully plastic solutions. The Δ*J* based on these two methods required the Ramberg-Osgood coefficient and strain hardening index as basic input to represent material tensile data. The disadvantage here is that Ramberg-Osgood fitting of the stress-strain curve can be seriously inaccurate, leading to inaccuracy in the estimated *J* [3, 4]. Additionally, while applying the GE/EPRI schemes for wide variety of test data of different crack geometries with wide range of material properties, it has been observed that GE/EPRI schemes highly over predict plastic Δ*J* in the elastic to fully plastic transition region

with respect to the incremental plasticity finite element solutions [5, 6]. In this study, the proposed ΔJ results will be compared with the one produced by the RSM. The estimate of ΔJ by the RSM in [7] is given by:

$$\Delta J = \Delta\sigma_{ref}\Delta\varepsilon_{ref}R \tag{2}$$

where

$$R = (\Delta K / \Delta\sigma_{ref})^2 \tag{3}$$

$$\Delta\sigma_{ref} = \sigma_y \Delta P / P_L \tag{4}$$

Here P_L is the limit load for the cracked geometry, and $\Delta\varepsilon_{\text{ref}}$ is the strain range corresponding to $\Delta\sigma_{\text{ref}}$ on the material cyclic stress-strain curve, which is given by the description of Ramberg-Osgood equation.

Another simplified ΔJ method was introduced by Dowling and Begley [8] on A533B steels, using an approximation of the *J*-integral based on the area under load–displacement curves—a simplified model proposed by Rice et al. [9]. ΔJ values calculated from load-displacement data were used [10] to correlate fatigue crack growth data in steels. ΔJ can be expressed by the potential energy change with crack growth as [11],

$$\Delta J = -\frac{1}{B}\left(\frac{d(\Delta U)}{da}\right) \tag{5}$$

where ΔU is the potential energy, B is the specimen thickness, and a is the crack length; ΔU is given by,

$$\Delta U = \int \Delta P d\delta \tag{6}$$

where ΔP is the loading amplitude and δ is the displacement. Thus, ΔU is an important factor in controlling the fatigue crack propagation [12].

Sumpter and Turner [13] expanded Equation (5) and rewrote it in the following form:

$$J = J_e + J_p \tag{7}$$

J_{e} and J_{p} are the elastic and plastic components, respectively, of the total J value from monotonic case, and can be expressed by the following equations:

$$J_e = \frac{\eta_e U_e}{B(W-a)} \tag{8}$$

$$J_p = \frac{\eta_p U_p}{B(W-a)} \tag{9}$$

where U_{e}, and U_{p} are the elastic and plastic components, respectively, of the total energy, η_{e}, and η_{p} are their corresponding elastic and plastic work factors, (W- a) is the ligament length and W is the specimen width. This unconventional approach to the *J*-integral, based on the potential energy approach was call ASTM standard method. Equation (8, 9) shows that J_{e} and J_{p} are a linear function of U_{e} and U_{p}.

[14-16] are the studies that investigated the behaviour of ΔJ with fatigue crack propagation for steels using load-displacement curves methods. It is important to notice that in all the studies mentioned above, ΔJ was calculated for each individual cycle. By adding the plastic contributions to the elastic terms and the plastic contributions are calculated using the areas under load–displacement curves. To date, the accumulated effects over the entire cycle have not been considered numerically. One of the purposes of this paper is to use a direct method to include these effects for calculating ΔJ.

The load–displacement curves approach (5) and ASTM standard methods (7-9) are selected in this study for the cyclic loading case, since the theoretical basis appears to be the best and permits easier processing of empirical data. Thus, the elastic–plastic cyclic *J*-integral is expressed as the summation of elastic and fully plastic solutions for various crack geometries and loading conditions which yield the following formula for estimating the total ΔJ value [17]:

$$\Delta J = \Delta J_e + \Delta J_p \tag{10}$$

Equation (5) and the form of ASTM show that ΔJ_e and ΔJ_p are a function of ΔU_e and ΔU_p, respectively. ie.

$$\Delta J_e = f(\Delta U_e) \qquad \Delta J_p = f(\Delta U_p) \tag{11}$$

where ΔJ_e and ΔJ_p are the elastic and plastic portion of ΔJ. And ΔU_e and ΔU_p are elastic and plastic strain energy respectively, as shown in the hysteresis loop of Fig.1, and their values will be calculated from Linear Matching Method (LMM) by accounting for the cumulative cycle effect.

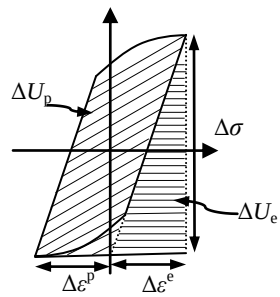

Fig.1 Hysteresis loop under cyclic loading case

The LMM is recognized as one of the most powerful methods among the direct methods [18, 19]. The LMM is distinguished from the other simplified methods by ensuring that equilibrium and compatibility are satisfied at each stage [18, 19]. The aim of this paper is to calculate the ΔJ through the extended version of LMM, which has a new capability to evaluate the stable cyclic response: the cyclic stresses, residual stresses, elastic & plastic strain energy and plastic strain ranges for the low cycle fatigue assessment with cyclic load history. By the use of this link, the cumulative cyclic effect of ΔJ can be solved.

In order to provide the energy form of ΔJ predictions, this work has been carried out on a single edge cracked plate subjected to cyclic tensile loading. This work has resulted in the formulation of a ΔJ estimation scheme using LMM which is the subject of coming sections of this paper. The scope of the study was:

(a) to obtain ΔJ_e vs ΔU_e and ΔJ_p vs ΔU_p relationships, using finite element computations, for a single edge cracked plate under cyclic tensile loading; the crack depth to plate depth ratios (a/W) used are 0.05, 0.075 and 0.1; the material models used are elastic perfectly plastic and Ramberg-Osgood model with the material work hardening exponent, n, with 5, 8 and 20;

(b) to formulate a ΔJ estimation scheme in energy form, based on the finite element results obtained in (a);

(c) to compare and validate the ΔJ estimation with the RSM result.

2. Numerical Procedures for Defining Elastic and Plastic Energy (ΔU_E and ΔU_P) Through LMM

2.1 Cyclic load history

Considering the following problem, a structure is subjected to a cyclic history of varying surface loads $P(x_k,t)$ acting over part of the structure's surface S_T. The variation is considered over a typical cycle $0 \le t \le \Delta t$ in a cyclic state. The remainder of the surface S, is denoted by S_u, and the displacement u_k=0.

Corresponding to these loading histories there is a linear elastic solution history;

$$\hat{\sigma}_{ij}(x_k,t) = \hat{\sigma}^{\Delta}_{ij}(x_k,t) \tag{12}$$

where $\hat{\sigma}^{\Delta}_{ij}$ denotes the varying elastic stresses due to $P(x_k,t)$.

2.2 Asymptotic cyclic solution

For the cyclic problem defined above, the stresses and strain rates will become asymptotic to a cyclic state where;

$$\sigma_{ij}(t) = \sigma_{ij}(t+\Delta t) \qquad \dot{\varepsilon}_{ij}(t) = \dot{\varepsilon}_{ij}(t+\Delta t) \tag{13}$$

The cyclic stress solution may be expressed in terms of two components, the varying elastic stress solution, and the associated changing residual stress field. The linear elastic solution (i.e. $\dot{\varepsilon}_{ij}^{P} = 0$) is denoted by $\hat{\sigma}_{ij}(x_k,t)$. The general form of the stress solution for the cyclic problems involving changing residual stress fields is given by;

$$\sigma_{ij}(x_k,t) = \hat{\sigma}_{ij}(x_k,t) + \rho_{ij}^{r}(x_k,t) \tag{14}$$

The ρ_{ij}^{r} is the changing residual stress during the cycle and it satisfies;

$$\rho_{ij}^{r}(x_k,0) = \rho_{ij}^{r}(x_k,\Delta t) = \bar{\rho}_{ij}(x_k) \tag{15}$$

where $\bar{\rho}_{ij}(x_k)$ is the constant element of ρ_{ij}^{r}.

2.3 Numerical procedure for the varying residual stress field and plastic strain range

The Linear Matching Method procedure for the assessment of residual stress history and the associated plastic strain range due to the cyclic component of the load history is described below in terms of N discrete time points. Following the same procedure as [20], for a strictly convex yield condition, the only instants when plastic strains can occur are at the vertices of the stress history $\hat{\sigma}_{ij}^{\Delta}(t_n)$, *n*=1 to *N*, where *N* represents the total number of time instants, t_1, t_2.....t_N, of the load extremes where plastic strain occurs and t_n corresponds to a sequence of time points in the load history. Then the plastic strain accumulated during the cycle $\Delta\varepsilon_{ij}^{T} = \sum_{n=1}^{N} \Delta\varepsilon_{ij}^{P}(t_n)$ where $\Delta\varepsilon_{ij}^{P}(t_n)$ is the increment of plastic strain that occurs at time t_n. The entire iterative procedure includes a number of cycles, where each cycle contains *N* iterations associated with *N* load instances. The first iteration is performed to evaluate the changing residual stress $\Delta\rho_{ij}^{1}$ associated with the elastic solution $\hat{\sigma}_{ij}^{\Delta}(t_1)$ at the first load instance. $\Delta{\rho_{ij}}_{m}^{n}$ is defined as the evaluated changing residual stress for *nth* load instance at *mth* cycle of iterations, where $n = 1,2,...N$ and $m = 1,2,...M$. At each iteration, the above changing residual stress $\Delta{\rho_{ij}}_{m}^{n}$ for *nth* load instance at *mth* cycle of iteration is calculated. When the convergence occurs at the *mth* cycle of iterations, the summation of changing residual stresses at N time points must approach to zero ($\sum_{n=1}^{N} \Delta{\rho_{ij}}_{M}^{n} = 0$) due to the stable cyclic response. Hence the constant element of the residual stress for the cyclic loading history is

$$\rho_{ij}^{r}(0) = \rho_{ij}^{r}(\Delta t) = \bar{\rho}_{ij} \tag{16}$$

and determined by

$$\bar{\rho}_{ij} = \sum_{n=1}^{N} \Delta{\rho_{ij}}_{1}^{n} + \sum_{n=1}^{N} \Delta{\rho_{ij}}_{2}^{n} + \cdots + \sum_{n=1}^{N} \Delta{\rho_{ij}}_{M-1}^{n} \tag{17}$$

The corresponding converged increment of plastic strain occurring at time t_n is calculated by

$$\Delta\varepsilon_{ij}^{p}(t_n) = \frac{1}{2\bar{\mu}_n}\left[\bar{\sigma}_{ij}^{\Delta'}(t_n) + \rho_{ij}^{'}(t_n)\right] \tag{18}$$

where $\bar{\mu}_n$ is the iterative shear modulus and notation (') refers to the deviator component of $\bar{\sigma}_{ij}^{\Delta}$ and ρ_{ij}.

$\rho_{ij}(t_n)$ is the converged accumulated residual stress at the time instant t_n, i.e.

$$\rho_{ij}(t_n) = \bar{\rho}_{ij} + \sum_{k=1}^{n} \Delta\rho_{ij}{}_M^k \tag{19}$$

The detailed iterative procedure for the evaluation of the residual stress history and associated plastic strain range has been implemented into ABAQUS through user subroutines UMAT and given in [20].

2.4 Numerical procedure for the elastic and plastic energy range

The total internal energy range under cyclic loading is given as:

$$\Delta U = \Delta U_e + \Delta U_p \tag{20}$$

where ΔU_e represents the linear elastic energy range as:

$$\Delta U_e = \int_V \frac{\Delta\sigma^2}{E} dV \tag{21}$$

where V corresponds to the total volume of the plate, and ΔU_p represents the plastic energy range as:

$$\Delta U_p = \int_{V_p} \Delta\sigma\Delta\varepsilon^p dV \tag{22}$$

Where V_p is corresponding to the plastic volume of the plate and the value of $\Delta\varepsilon^p$ is obtained from equation (18)

3. Numerical Example

3.1 Geometry and material model

The material properties of the single edge cracked plate are yield stress, σ_y=700 MPa, Poisson's ratio, v=0.3, Young's modulus, E= 200 GPa and its geometrical shape is shown in Fig.2a. For non-linear analysis, the elastic perfectly plastic and Ramberg-Osgood types of material model are adopted in this study. The following Ramberg-Osgood type stress-strain relationship for the form of monotonic loading is [22]:

$$\varepsilon = \frac{\sigma}{E} + \frac{\alpha}{E}\left(\frac{1}{\sigma_0}\right)^{n-1}\sigma^n \tag{23}$$

where ε is the total strain, σ is the applied stress, E is the elastic modulus, σ_0 is reference stress usually taken as 0.2% yield stress (σ_y), and α and n are the Ramberg-Osgood plastic hardening constants. This can be converted to fatigue loading using stress and strain ranges as:

$$\Delta\varepsilon = \frac{\Delta\sigma}{E} + 2\frac{\alpha}{E}\left(\frac{\Delta\sigma}{2\sigma_0}\right)^n\sigma_0 \tag{24}$$

where $\Delta\sigma$ is the true stress range, $\Delta\varepsilon$ is the true strain range. At the lower limit, n=1, the above equation represents linear-elastic behaviour, and at the upper limit, n=∞, it may be represented as an elastic-perfectly plastic behaviour. The first term on the right-hand side of the above equation presents the elastic part and the second term presents the plastic part.

Then the plastic strain amplitude from equation (24) can be written as:

$$\Delta\varepsilon_p = 2\frac{\alpha}{E}\left(\frac{\Delta\sigma}{2\sigma_0}\right)^n\sigma_0 \tag{25}$$

and

$$\alpha = \frac{\Delta\varepsilon_p E}{2\sigma_0}\left(\frac{2\sigma_0}{\Delta\sigma}\right)^n \tag{26}$$

In this study the reference stress (σ_0) is taken as 0.2% yield stress (σ_y), where σ_y is defined as half the stress

range that results from a strain range of 0.2% in the steady state as:

$$\sigma_y = \frac{\Delta\sigma_{0.2\%}}{2} \quad \Delta\varepsilon_p = 0.2\% \tag{27}$$

From equations (25, 26), α can be evaluated with given yield stress (σ_y) as:

$$\alpha = \frac{0.2\%E}{2\sigma_0} \tag{28}$$

From equation (28) it is important to note that when $\sigma_0=\sigma_y$, α is independent of the Ramberg-osgood plastic hardening constant n.

The elastic perfectly plastic and the Ramberg-Osgood material model with power hardening exponents in equation (24) n=5, 8, 20, and the crack length ratio a/W=0.05, 0.075, 0.1 are used to develop the ΔJ estimation scheme and to illustrate the features of the ΔJ vs. potential energy curves. All models have an aspect ratio L/W=4. Fig.2c shows the curves of the above mentioned material constitutive relations.

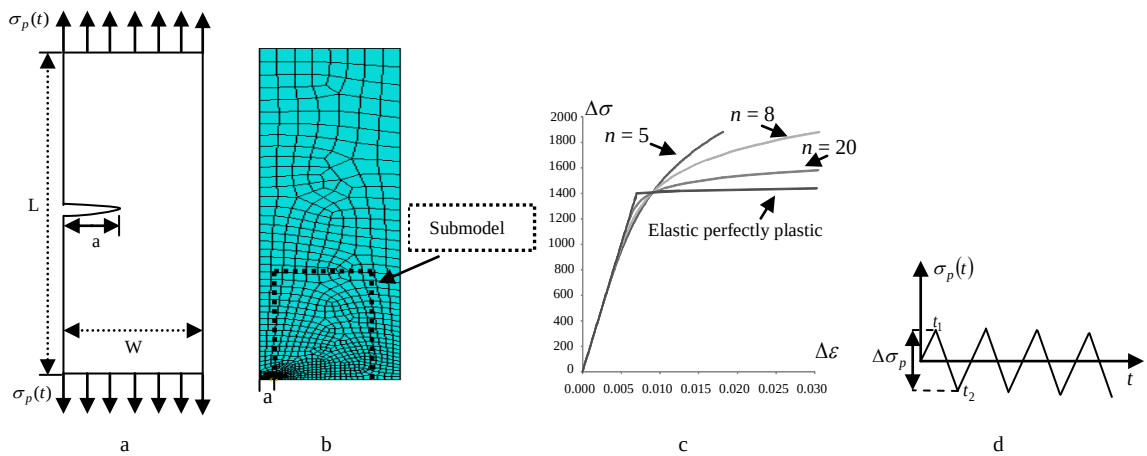

Fig.2 (a) Single edge cracked plate subjected to cyclic tensile loading (b) Global FEM and relative sub model (c) The curve of constitutive relation for elastic perfectly plastic and Ramberg-Osgood material model with different hardening n (d) The cyclic tensile loading history with tension range $\Delta\sigma_p$

3.2 Loading

The single edge cracked plate is subjected to cyclic tension loading under plane strain condition. The detailed cyclic loading histories are given in Fig.2d, which shows a cyclic loading history with two load extremes during each load cycle. The two extremes of loading history (Fig.2d) can be formulated as $\sigma_p(t_1)=\Delta\sigma_p/2$ and $\sigma_p(t_2)=-\Delta\sigma_p/2$, respectively, where $\Delta\sigma_p$ represents the tension range. The reference tensile loading range with loading magnitude equal to 100MPa is used in cyclic tension cases.

3.3 The global finite element model

Half-model is required for the cyclic tensile loading condition, as shown in Fig.2b. The boundary condition is imposed in the FEM and rigid body motion for the cracked plate is prevented by restraining the two degrees of freedom of the corner node opposite the cracked face. Because the ΔJ includes energy type terms within a relatively remote boundary encompassing the crack tip, it is not necessary to use special elements to account for the stress singularity at the crack tip. Thus, the analysis is performed using ABAQUS type CPE8R 8 node quadratic quadrilateral elements with reduced integration scheme.

3.4 The submodeling

Recently, the submodeling technique has often been used in the FE numerical analysis to study in detail an area of interest in a model. Herein, the area of interest is the region of high stress caused by the individual crack as shown in Fig.2b. The main idea of the submodeling technique is to perform a global-local transition. This approach gives an opportunity to make a local mesh refinement, since as the submodel region has a finer mesh, a submodel can provide an accurate, detailed solution. Besides better accuracy, another advantage is that one can avoid the other high stress fields caused by other stress risers, i.e., boundary conditions. In order to investigate the dependence of the cyclic *J*-integral results on the submodel size, five different submodel size ratios are considered in this study, which are A_{sub1}/A_{Global}=0.015, 0.05, 0.13, 0.24, 1.0.

4. An Analysis of Energy Form Expressions for Δ*J*

This section presents the derivation of a Δ*J* expression from FEA simulations. The *J* value from ABAQUS is composed of elastic, J_e, and plastic, J_p, parts. However, these values provided by ABAQUS are only valid for the monotonic case, and there is no Δ*J* value account for the cyclic loading case from ABAQUS. A reasonable approximation to obtain the values of Δ*J* can be achieved by performing a monotonic loading calculation, but with σ_y replaced by $2\sigma_y$ [23, 24]. This conclusion was also examined by Chen at el. [25] that discovered that in an un-cracked body subjected to variable loading conditions, the variations between such a monotonic loading solution with an equivalent cyclic solution, measured after a reasonable number of loading cycles, is relatively small. The above assumption could be explained by Fig.3, which shows the maximum principle strain range for cyclic tensile loading with a/W=0.075 and submodel size A_{sub4}.

Both monotonic and cyclic loading cases have similar maximum principal plastic strain range at the crack tip, as observed in Fig.3. Then using such an assumption, Δ*J* values for two-dimensional elastic-plastic finite element analyses under fatigue loading are then identified or replaced by the *J*-integral values for the monotonic loading by employing the finite element package ABAQUS.

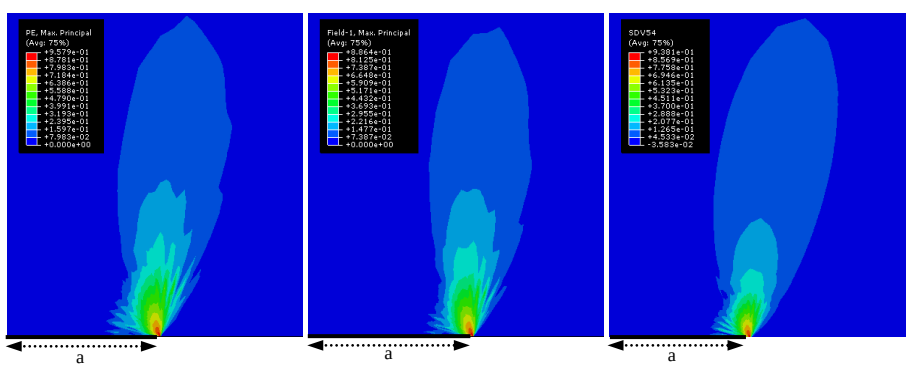

a b c

Fig.3 Maximum principal plastic strain for a single edge cracked plate subjected to cyclic tensile loading with a/W = 0.075 (a)ABAQUS result from monotonic case (b)ABAQUS result from step-by-step cyclic loading case (c)LMM result for cyclic loading case

From Figs.3b-3c, it is observed that the LMM solution gives better results than the step-by-step cases provided from ABAQUS comparing to the monotonic one. The reason for the poorer results of the step-by-step inelastic analysis may be since while conducting the analysis, the cyclic response values do not reach the steady cyclic state. Past investigations have revealed that the conduction of such solutions requires relatively long analysis times. In order to simplify the calculations, the cyclic solutions (i.e. ΔU_e and ΔU_p) from LMM are adopted for the coming sections. In the following sections, the relationship between ΔJ_e, ΔU_e and ΔJ_p, ΔU_p will be introduced.

4.1 Formulation of ΔJ_e using submodeling

The elastic portion, ΔJ_e, can be calculated from the relationship between ΔJ^* and $\Delta U^*/A_{sub}$, where ΔJ^* and $\Delta U^*/A_{sub}$, represent the cyclic *J*-integral and potential energy rate from the linear elastic material model, respectively.

4.1.1 The relationship between ΔJ^* and $\Delta U^*/A_{sub}$: As observed from Fig.4a, ΔJ^* is a linear function of $\Delta U^*/A_{sub}$ for the linear elastic material model, which is independent of the submodel sizes. This relationship can be formulated as:

$$\Delta J^* = C\frac{\Delta U^*}{A_{sub}} \tag{29}$$

where, *C* is the rate at which ΔJ^* increases with the elastic energy rate $\Delta U^*/A_{sub}$.

4.1.2 The relationship of $\Delta U^*/A_{sub}$ and $\Delta U_e/A_{sub}$ using submodeling: In order to calculate ΔJ_e for inelastic material model by applying the same form as ΔJ^*. The value of $\Delta U^*/A_{sub}$ and $\Delta U_e/A_{sub}$ are being compared with elastic perfectly plastic and Ramberg Osgood material model where $\Delta U_e/A_{sub}$, is the elastic potential energy rate from those inelastic material models. Fig.4b shows the variations of the difference in $\Delta U^*/A_{sub}$ and $\Delta U_e/A_{sub}$ with the increasing submodel size from A_{sub1} to A_{sub5}. It is observed from Fig.4b that the values of $\Delta U^*/A_{sub}$ and $\Delta U_e/A_{sub}$ are the same and not affected by the types of material model with the same submodel size and with all load levels up to the limit load. As it may be observed from Figs.4a-4b, the results of elastic portion of cyclic *J* and the potential energy rate obtained by the submodel size equal to A_{sub1} deviate significantly compared to the others. This phenomenon could be explained by Fig.5a.

Fig.5a shows the equivalent plastic strain range with different submodel sizes and with applied cyclic loading *P*=1000Mpa.

In Fig.4b, it is observed that the results of elastic strain energy rate from the submodel sizes A_{sub1} and A_{sub2} have different values than the other submodel sizes. These differences become larger with increasing applied loading by comparing to the other submodel sizes. As observed from Fig.5a, for the load levels equal to 85% of limit load, the submodel sizes equal to A_{sub1} and A_{sub2} are not sufficiently large to cover the plastic strains zone occuring on the global model. The values of $\Delta U^*/A_{sub}$ and $\Delta U_e/A_{sub}$ are stabilized for the submodel size equal to A_{sub3}-A_{sub5} (Fig.4b) for the load levels up to the limit load, since these sizes cover the plastic strains zone caused by the individual crack (Fig.5a). Figs.4b-5a also show that the elastic potential rate is stabilized for the range of submodel size ratio (A_{sub} /A_{Global}) from 0.13 to 1.

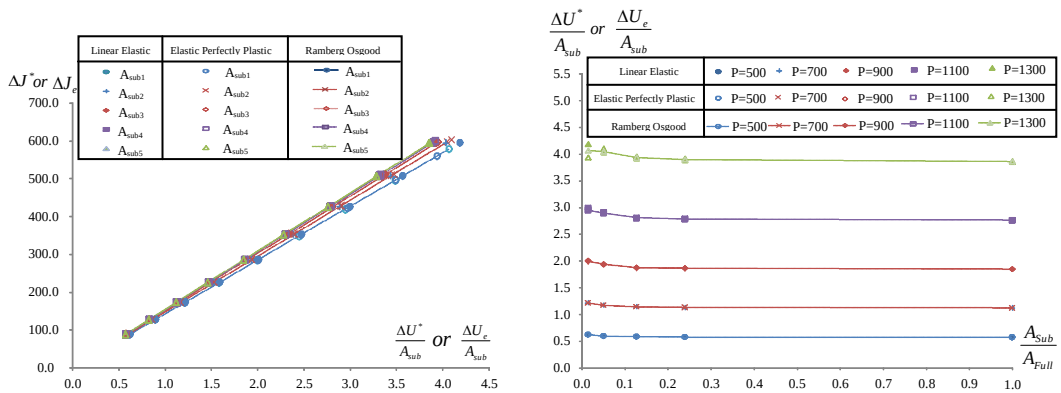

Fig.4 (a) The relationship between elastic cyclic *J* and elastic energy rate with different types of material model and submodeling size ratio (b) The relationship between elastic energy rate and submodelling size ratio for different types of material model with all loads up to limit load

4.1.3 The submodeling boundary: From the above results it can be concluded that for the single edge cracked plate under cyclic tensile loading case, the submodel boundaries should be taken far from the crack tip, so that the stress field in the boundary is completely unaffected by the crack. This means that the selected boundary should be able to surround the plastic zone completely, i.e., including the total plastic energy ΔU_p caused by the individual crack only.

4.1.4 The relationship between ΔJ_e and $\Delta U_e/A_{sub}$: From the relationship between $\Delta U^*/A_{sub}$ and $\Delta U_e/A_{sub}$, the elastic portion, ΔJ_e from the inelastic material model can be calculated using the linear solution C, and the elastic energy ΔU_e from elastic-plastic solution as:

$$\Delta J_e = C\frac{\Delta U_e}{A_{sub}} \tag{30}$$

Equation (30) is established on the assumptions that ΔJ_e is a linear function of $\Delta U_e/A_{sub}$ (Fig.4a), and C is the slope of the lines calculated from linear elastic material. This equation is independent of the material model that is considered in this study.

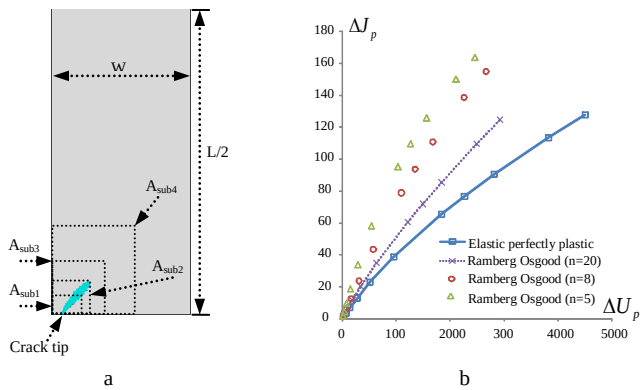

Fig.5 (a) The equivalent plastic strain range with different submodelling sizes for elastic perfectly plastic material model at P=1100 MPa (b) The relationship between plastic cyclic J and plastic energy for different types of material model

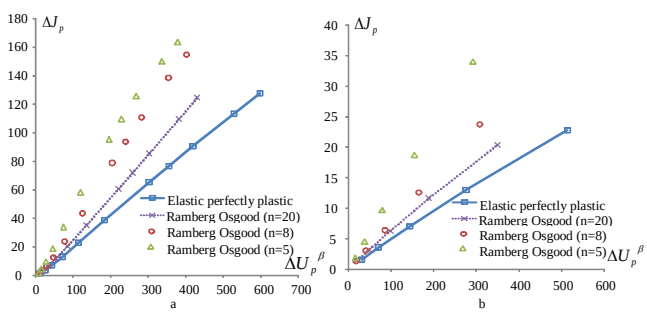

Fig.6 The relationship between plastic cyclic J and plastic energy for different types of material model (a) with β=3/4 (b) with β=1

4.2 Formulation of ΔJ_p

The plastic portion, ΔJ_p, can be expressed in terms of ΔJ and ΔJ_e as:

$$\Delta J_p = \Delta J - \Delta J_e \tag{31}$$

As described in the previous section, the submodeling boundary should include the plastic zone induced by the crack. Therefore, the value of ΔU_p for the individual crack is independent of these submodeling sizes. The

variation of ΔJ_p with ΔU_p , for elastic perfectly plastic and Ramberg Osgood material model with the applied loading up to limit load is shown in Fig.5b. Fig.5b also shows that the increase in ΔJ_p values for Ramberg Osgood and elastic perfectly plastic material model seem to have a linear variation with increasing ΔU_p. By plotting ΔJ_p against the power formulation of ΔU_p^{β} for a/W=0.075 (Fig.6), an approximate linear relationship is established which can be expressed as:

$$\Delta J_p = D(\Delta U_p)^{\beta} \tag{32}$$

where D, the slope of the lines in Fig.6, is a function of geometric, material model and has to be determined. The power index β is included to form the linear relationship of ΔJ_p. In Fig.6a β is chosen as 3/4 for all inelastic material models that are considered in this study. As well known, if the plastic zone size is less than about 10% of the crack length, small-scale yielding conditions exist around the crack tip. Fig.6b shows variation of ΔJ_p with ΔU_p^{β} (with β=1) for different inelastic material model with the plastic zone size up to 50% of the crack length. It is observed from Fig.6b that ΔJ_p is a linear function of ΔU_p^{β} (with β=1) for cyclic tensile loading case with different inelastic material model. Therefore, within the region of the plastic zone size, up to 50% of the crack length, equation (32) can be rewritten as,

$$\Delta J_p = D(\Delta U_p)^{1} \tag{33}$$

Equation (33) has the same formulation as the ASTM ones (9), which is established on the assumptions that ΔJ_p is a linear function of ΔU_p.

4.3 Formulation of ΔJ

It can be concluded from the above discussion that for the single edge cracked plate under cyclic tensile loading, the cyclic J integral, ΔJ, can be expressed as,

$$\Delta J = C\frac{\Delta U_e}{A_{sub}} + D(\Delta U_p)^{\beta} \tag{34}$$

β=1, for plastic zone size up to 50% of the crack length.

5. Proposed ΔJ Estimation for Single Edge Cracked Plate

5.1 Determination of C

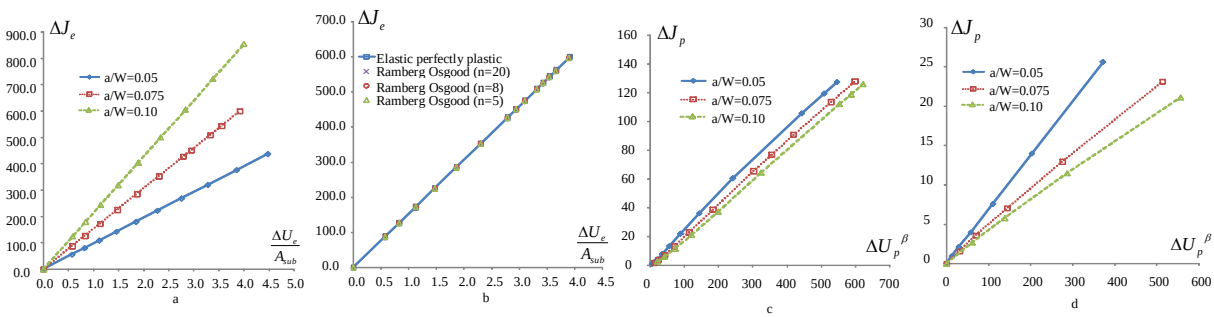

Fig.7 (a) The relationship between ΔJ_e and $\Delta U_e/A_{sub}$ for elastic perfectly plastic material model with different crack size ratio (b) The relationship between ΔJ_e and $\Delta U_e/A_{sub}$ for different material constitutive model with a/W=0.075 (c) The relationship between plastic cyclic J and plastic energy, for different crack length ratio with β=3/4 (d) with β=1

In order to determine the formulation of function C from the ΔJ_e values, the variation of ΔJ_e with $\Delta U_e/A_{sub}$ for three a/W ratios with elastic perfectly plastic material model and for different inelastic material model with

a/W=0.075 are examined by plotting ΔJ_e against $\Delta U_e/A_{sub}$ respectively as shown in Fig.7a and Fig.7b. In Fig.7a and Fig.7b the size of the submodel is equal to A_{sub4}. It is observed from Fig.7a and Fig.7b that the dimensionless parameter C is independent of the inelastic material model, and is a function of a/W ratio only. Therefore, slope C is a function of $f(a/W)$ and is formulated as,

$$C = f\left(\frac{a}{W}\right) \tag{35}$$

where $f(a/W)$ is the influence function for the crack ratio range.

In order to find this influence function, the slope of ΔJ_e is replotted in graphs of function $f(a/W)$ against a/W, as shown in Fig.8a. Trend lines are fitted to the data obtained from the ΔJ_e result of different crack ratios to show the influence function. Equation (36) is the obtained from the influence f **Keywords:** cyclic J integral, Linear Matching Method, single edge cracked plate

unction for the slope C.

$$f\left(\frac{a}{W}\right) = 2314\left(\frac{a}{W}\right) - 19.11 \tag{36}$$

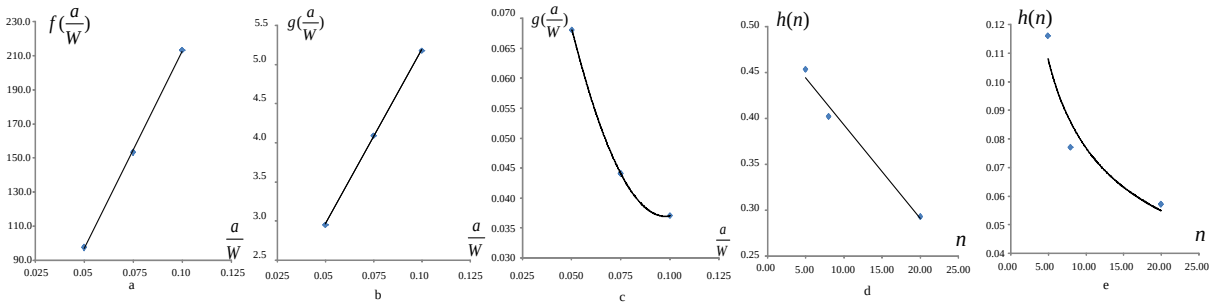

Fig.8 (a) Influence function $f(a/W)$ for slope C against crack length ratio (b) Influence function $g(a/W)$ for slope D against crack length ratio for β=3/4 (c) for β=1 (d) Influence function $h(n)$ for slope D against Ramberg-Osgood material hardening n with β=3/4 (e) with β=1

5.2 Determination of D

In order to determine the formulation of function D from the ΔJ_p values, the variation of ΔJ_p with ΔU_p^{β} for three a/W ratios with elastic perfectly plastic material model is examined by plotting ΔJ_p against ΔU_p^{β} for β=3/4 and β=1 as shown respectively in Fig.7c and Fig.7d.

It is observed from Fig.6 and Figs.7c-7d that the slope D is a function of a/W ratio and inelastic material model for different β values.

In order to simplify the formulation, slope D is assumed to be the product of two independent functions g(a/W) and h(n). Therefore, parameter D is formulated as,

$$D = \frac{g\left(\frac{a}{W}\right)h(n)}{aB} \tag{37}$$

Where a is the crack length, B is the thickness of the plate, and $g(a/W)$, $h(n)$ are the influence functions for the crack length ratio range and the inelastic material model.

In order to find these influence functions, the results of ΔJ_p are replotted in graphs of functions g and h against a/W and n respectively as shown in Figs.8b-8e for β=3/4 and β=1. Trend lines are fitted to the data obtained from the results of ΔJ_p vs ΔU_p^{β} for different crack length ratios and inelastic material model with β=3/4 and β=1, to show the influence function.

Equations (38) and (39) are the obtained influence functions for the crack length ratios ranging from β=3/4 to β=1, respectively. Equations (40, 41) and (42, 43) are the obtained influence functions for the inelastic

material model range for β=3/4 and β=1, respectively.

Once C and D are defined, the cyclic J integral value is calculated for the single edge cracked plate under cyclic tensile loading mentioned in this study.

For β=3/4

$$g\left(\frac{a}{W}\right)=44.5\left(\frac{a}{W}\right)+0.733 \tag{38}$$

For β=1

$$g\left(\frac{a}{W}\right)=13.6\left(\frac{a}{W}\right)^{2}-2.66\left(\frac{a}{W}\right)+0.167 \tag{39}$$

For β=3/4

With Ramberg Osgood parameter material n ranging from 5-20

$$h(n)=-0.010(n)+0.495 \tag{40}$$

with elastic perfectly plastic material model

$$h(n)=0.218 \tag{41}$$

For β=1

With Ramberg Osgood parameter material n ranging from 5-2

$$h(n)=0.236(n)^{-0.48} \tag{42}$$

with elastic perfectly plastic material model

$$h(n)=0.043 \tag{43}$$

6. Validation and Discussion of the Estimation Scheme

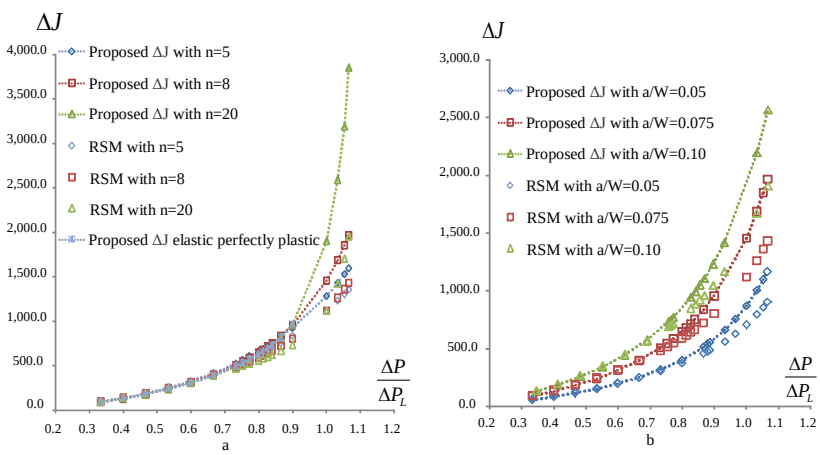

Fig.9 Comparison of the RSM and proposed ΔJ: (a) with different types of material model (b) with different crack length ratio

In this section we will consider first the constitutive relation of a cracked plate with different Ramberg-Osgood material. The ΔJ equation is obtained in section 5, for single edge cracked plate loaded in cyclic tension. The results obtained from the ΔJ equation are compared graphically with Reference Stress Method, with different Ramberg-Osgood parameter n. Fig.18a shows that the variation of ΔJ with Ramberg-Osgood material, against load ratio $\Delta P/\Delta P_L$, where ΔP_L is the limit load range for the cyclic tensile loading, with a/W=0.075. Good agreement is obtained between the proposed ΔJ equation and RSM results when the load ratio is smaller than 1.0. As the load ratio is greater or equal to 1.0 the difference of ΔJ between the proposed method and RSM becomes very significant, and this difference gets larger with the increasing number of Ramberg-Osgood parameter n. Fig.9a also shows that for the load ratio smaller than 1.0, the values of ΔJ drop with the increasing number of n, and for the load ratio greater or equal to 1.0, the values of ΔJ rise with increasing number of n for both proposed ΔJ method and RSM. This phenomenon can be explained by the curves of the material constitutive relations shown in Fig.2c. For the stress range less than twice of yield stress, the product of total stress-strain range is decreasing with increasing of n. And, for the stress range greater than twice of yield stress, the product of total stress-strain range is increasing with increasing of n.

Fig.9b shows the variation of ΔJ against load ratio $\Delta P/\Delta P_L$ for different crack depth with Ramberg-Osgood material n=8. Good agreement of the proposed ΔJ equation and RSM solutions is exhibited when the load ratio smaller than 1.0. For load ratio greater or equal to 1.0, the results deviate significantly.

7. Conclusions

In this study, a general ΔJ calculation method based on the LMM is proposed. The estimation scheme for single edge cracked plate under cyclic tensile loading is developed. The following conclusions can be drawn from this study:

1. The proposed ΔJ estimation, primarily derived from fracture mechanics concepts, is now considered from direct method though LMM, which includes the cumulative effects over the cycle. The calculated values of ΔJ with the applied loading up to limit load are shown to correlate well with RSM under cyclic tensile loading.
2. ΔJ_e is a linear function of $\Delta U_e / A_{sub}$, and this relation is independent of the material models that are considered in this study.
3. ΔJ_p is a linear function of ΔU_p^{β}. When β=1, this relation reduced to small scale yielding condition with the region of the plastic zone size up to 50% of the crack length.
4. The hardening constant n for Ramberg-Osgood model has little effect on the values of ΔJ when the cyclic loading ratio ($\Delta P/\Delta P_L$) is less than 1.0
5. A rapid procedure for predicting the values of ΔJ is provided for single edge cracked plate under cyclic tensile loading case.

Acknowledgements

The authors gratefully acknowledge the support of the Engineering and Physical Sciences Research Council (EP/G038880/1) of the United Kingdom, and the University of Strathclyde during the course of this work.

References

[1] N. E. Dowling and J. A. Begley. Fatigue crack growth during gross plasticity and the J-integral. ASTM-STP WI. 1976; 82-103.
[2] P. Pairs and F Erdogan. A critical analysis of crack propagation laws. J. Basic Engng. 1963; 85: p.528-534.

[3]Chattopadahyay J. Improved J and COD estimation by GE/EPRI method in elastic to fully plastic transition zone. Eng. Fract. Mech. 2006; 73. 1959-1979.

[4]A.G. Miller, and R.A. Ainsworth. Consistency of numerical results for power law hardening materials and the accuracy of the reference stress approximation. Eng Fract Mech. 1989; 32. 237-247

[5]Zahoor A. Evaluation of J-integral estimation schemes for flawed throughwall pipes. Nucl Engng Des. 1987; 100. 1–9.

[6]Kim Yun-Jae, Huh Nam-Su, Kim Young-Jin. Effect of Lu¨ders strain on engineering crack opening displacement estimations for leak before break analysis finite element study. Fatigue Fract Engng Mater Struct. 2001; 24. 617–24.

[7]R. A. Ainsworth, M.B. Ruggles, Y. Takahashi. Flaw assessment guide for high temperature reactor components subject to creep fatigue loading. Eng. Technology Divison. 1990.

[8]Dowling NE, Begley JA. Fatigue crack growth during gross plasticity and the J-integral. Mechanics of crack growth. ASTM STP 590. Philadelphia. PA: American Society for Testing and Materials. 1976; 82–103.

[9]Rice JR, Paris PC, Merkle JG. Some further results of J-integral analysis and estimates. Progress in flaw growth and fracture toughness testing. ASTM STP 536. Philadelphia, PA. American Society for Testing and Materials. 1973; 231–45.

[10]Brose WR, Dowling NE. Size effects on the fatigue crack growth rate of type 304 stainless steel. In: Landes JD, Begley JA, Clarke GA, editors. Elastic–plastic fracture. ASTM STP 668. Philadelphia, PA: American Society for Testing and Materials. 1979; 720–35.

[11]Y. Lambert, P. SaiBard aud C. Bathias. Application of the J concept to fatigue crack growth in large-scale yielding. ASTM STP 969. 1988; 318-329.

[12]Y. Izumi and M. E. Fine. Role of plastic work in fatigue crack propagation in metals, Engineering Fracture Mechanics I1. 1979; 791-804.

[13]J.D. Sumpter, C.E. Turner. Int. J. Fract. 1973; 9: 320.

[14]Wang S-Z, Yang Z, Kang M-K. Fatigue crack growth rate under full yielding condition for 15CDV6 steel. Engng Fract Mech1983; 18(4). 895–902.

[15]El-Haddad MH, Mukherjee B. Elastic–plastic fracture mechanics analysis of fatigue crack growth. In: Shih CF, Gudas JP, editors. Elastic–plastic fracture: second symposium, vol. II—fracture resistance curves and engineering applications. ASTM STP 803. Philadelphia. PA: American Society for Testing and Materials. 1983; 689–707.

[16]Tanaka K, Hoshide T, Nakata M. Elastic–plastic crack propagation under high cyclic stresses. In: Shih CF, Gudas JP, editors. Elastic–plastic fracture: second symposium, vol. II—fracture resistance curves and engineering applications. ASTM STP 803. Philadelphia. PA: American Society for Testing and Materials. 1983; 708–722.

[17]J. Chattopadhyay. Improved J and COD estimation by GE/EPRI method in elastic to fully plastic transition zone. Engineering Fracture Mechanics. 2006; 73:1959–1979.

[18]Ponter, A.R.S, & Chen, H.F. A minimum theorem for cyclic load in excess of shakedown, with application to the evaluation of a ratchet limit. European Journal of Mechanics - A/Solids. 2001; 20:539-553.

[19]Chen HF, Ponter ARS. A method for the evaluation of a ratchet limit and the amplitude of plastic strain for bodies subjected to cyclic loading. European Journal of Mechanics - A/Solids. 2001; 20: 555-571.

[20]Chen, H.F. & Ponter, A.R.S. Linear Matching Method on the evaluation of plastic and creep behaviours for bodies subjected to cyclic thermal and mechanical loading. International Journal for Numerical Methods in Engineering. 2006; 68:13-32.

[21]C. L. Lau, M. M. K. Lee, A. R. Luxmoore. Mythologies for predicting J-integrals under large plastic deformation-I. further developments for tension loading. 1994; 49: 337-554.

[22]ABAQUS. User's manual. Version 6.7. 2007;

[23]J.R. Rice. in ASTM STP 415. 1967; 242-311.

[24]N.E. Downling. Crack growth during low-cycle fatigue of smooth axial specimens. Cyclic-stress-strain and plastic deformation aspects of fatigue crack growth. ASTM STP. 1997; 637: 97-121.

[25]H.F. Chen, A. R. S. Ponter. A method for the evaluation of a ratchet limit and the amplitude of plastic strain for bodies subjected to cyclic loading. European Journal of Mechanics and Applied Solids. 2001; 20: 555-571.